Nanoscale

PAPER

View Article Online
View Journal | View Issue

Cite this: *Nanoscale*, 2020, **12**, 7072

Stimuli-responsive graphene-based hydrogel driven by disruption of triazine hydrophobic interactions†

Jorge Leganés,[a,b] Ana Sánchez-Migallón,[a,b] Sonia Merino *[a,b] and Ester Vázquez *[a,b]

Received 14th December 2019,
Accepted 26th February 2020

DOI: 10.1039/c9nr10588c

rsc.li/nanoscale

The study reported here concerns the preparation of a novel graphene-diaminotriazine (G-DAT) nanocomposite hydrogel for application in the drug delivery field. The hybrid nature of this material is founded on two key elements: the presence of the DAT backbone induced the formation of hydrophobic regions that allowed efficient loading of a series of drugs of increasing hydrophobicity (Metronidazole, Benzocaine, Ibuprofen, Naproxen and Imipramine), while simultaneously endowing swelling-induced pH-responsiveness to the hydrogel. Additionally, the incorporation of graphene was found to interfere with these hydrophobic domains through favourable non-covalent interactions, thus leading to the partial disruption of these aggregates. As a consequence, graphene facilitated and enhanced the release of model hydrophobic drug Imipramine in a synergistic manner with the pH trigger, and increased the swelling capacities and improved mechanical performance. This hybrid hydrogel can therefore be envisaged as a proof-of-concept system for the release of hydrophobic compounds in the field of drug delivery.

Introduction

Macromolecular hydrogels are three-dimensional crosslinked polymer networks that are able to swell and incorporate high contents of water. The water-insolubility, biocompatibility, biodegradability or bioadhesivity of these materials allow them to mimic closely natural tissue.[1,2] In particular, these materials have been in the spotlight of drug delivery techniques due to their ability to offer spatial and temporal control over the release of therapeutic agents.[3] However, hydrogels have been limited to the delivery of water-soluble compounds since their nature is intrinsically hydrophilic,[4] which also leads to inefficient hydrophobic drug loading. Several strategies have been implemented to address these issues, such as the introduction of hydrophobic polymer blocks,[5] or the inclusion of cyclodextrins (CD).[6,7]

An alternative strategy would be to focus on tailoring hydrophobic microenvironments into hydrophilic networks by the formation of non-covalent interactions. In this respect, 1,3,5-triazine rings are useful structures that form a variety of different host–guest interactions[8] and, among these systems, diaminotriazines (DAT) stand out due to their ability to establish strong intermolecular hydrophobic interactions. Maly *et al.*[9] were the first to observe that 4,6-diamino-1,3,5-triazines self-associate in solution into disc-like hydrogen-bonded rosettes and columnar mesophases by stacking of an extended aromatic core. Asanuma *et al.*[10] demonstrated that DAT residues present in the homopolymer poly(2-vinyl-4,6-diamino-1,3,5-triazine) (PVDT) afforded apolar microenvironments through π–π stacking between hydrophobic DAT–DAT segments, a situation that contributed to the strong absorption of nucleotides through molecular recognition. The versatility of these interactions encouraged an expansion of the scope of DAT-based macrostructures to the delivery of bioactive compounds, particularly for use in gene transfection.[11–13] In this respect, Wang *et al.* fabricated a nucleoside-responsive DAT-based hydrogel that was capable of releasing a model drug in response to thymine upon cleavage of DAT hydrogen bonds,[14] thus demonstrating that these hydrogels may be considered as stimuli-responsive delivery carriers.

Graphene is a state-of-the art nanomaterial that consists of a honeycomb 2D lattice in which sp^2-carbon atoms delocalise the π-electron cloud, the quality of which imparts the material with extraordinary features.[15,16] From a chemical point of view, pristine graphene offers numerous possibilities for non-covalent functionalisation with a variety of molecules, ranging from small drugs[17] to polymeric matrices.[18] In this respect,

[a]*Instituto Regional de Investigación Científica Aplicada (IRICA), 13071 Ciudad Real, Spain*
[b]*Facultad de Ciencias y Tecnologías Químicas, Universidad de Castilla-La Mancha (UCLM), 13071 Ciudad Real, Spain. E-mail: ester.vazquez@uclm.es*

†Electronic supplementary information (ESI) available. See DOI: 10.1039/c9nr10588c

we demonstrated particularly favourable π–π interactions between melamine (2,4,6-triamino-1,3,5-triazine) and few-layer graphene.[19,20] In this case, melamine was observed to form a uniform thin coating on the top of graphene surface: the triazine derivative was found to establish π–π interactions between the aromatic nucleus and the graphenic surface, while extended 2D networks of triazine molecules were formed due to the presence of hydrogen bonds, which in turn reduced van der Waals forces between the graphene layers. This "exfoliating effect" of melamine played a decisive role in the mechanochemical treatment employed to obtain good-quality non oxidized graphene.[21]

The low tolerance of delivery systems for drugs with poor water solubility still remains the main challenge in the precise release of marketed drugs. We envisaged that the introduction of diaminotriazine residues into graphene-based hydrogels would open up new alternative routes to hydrophobic drug delivery. The non-covalent nature of DAT-based hydrogels endows hydrophobicity as well as stimuli-responsiveness,[22,23] both of which are requisites for these applications. On the other hand, we previously observed that graphene interacts favourably with DAT thin films through π–π and NH_2-graphene interactions and combination of the two aforementioned elements may make graphene-diaminotriazine (G-DAT) hybrid hydrogels useful platforms for the controlled release of hydrophobic drugs. These proof-of-concept hydrogels may expand the scope of drug delivery by means of non-covalent interactions.

Experimental section

Materials and reagents

Poly(ethylene glycol) methyl ether methacrylate (OEGMA, M_n = 950), acrylamide (AM), *N*,*N*′-methylenebis(acrylamide) (MBA), potassium peroxydisulfate (KPS), Metronidazole (MZ), Ibuprofen (IB), Epichlorohydrin (EPI), odium disulfide, melamine and PBS (phosphate buffered saline, pH = 7.4) were purchased from Sigma-Aldrich as reagent-grade materials. Benzocaine (BZ), Naproxen (NX), Imipramine hydrochloride (IMI) and 2,4-diamino-6-[2-(2-methyl-1-imidazolyl)ethyl]-1,3,5-triazine (2MA) were purchased from TCI chemicals. Graphite powder was acquired from Bay Carbon Inc. (SP-1 reference). SGF (simulated gastric fluid) was prepared from a 0.063 M solution of HCl.

Preparation of 2-vinyl-4,6-diamino-1,3,5-triazine (VDAT)

The synthesis of VDAT was carried out according a patented procedure.[24] In a typical procedure, 2,4-diamino-6-[2-(2-methyl-1-imidazolyl)ethyl]-1,3,5-triazine (2MA, 0.17 mol) was suspended in 75 mL deionized water with stirring. Epichlorohydrin (EPI, 0.17 mol) and sodium disulfide (1.7.10–3 mol) were added and the mixture was heated under reflux for 3 hours. The crude product was filtered off and washed with 250 mL of cold water. The product was filtered under vacuum and dried in a desiccator for 2 days to give a pure colourless solid. Yield: 54%. ^{1}H-NMR: s (6.64 ppm, 4H), dd (6.4 ppm, 1H, *J*3 = 17.3 Hz), dd (6.3 ppm, 1H, *J*3 = 17.3 Hz) dd (5.62 ppm, 1H, *J*3 = 10.1 Hz).

Preparation of DAT hydrogels

The synthesis of DAT hydrogels was carried out by *in situ* radical polymerisation in DMSO. VDAT (150 mg mL^{-1}), OEGMA (135 mg mL^{-1}), AM (135 mg mL^{-1}), cross-linker MBA (2 mg mL^{-1}) and KPS initiator (2 mg mL^{-1}) were dissolved with stirring. The mixture was sonicated prior to casting into pre-heated silicon moulds (1 cm × 0.5 cm) at 70 °C in an oven for 20 min. The resultant organogels were washed thoroughly in 600 mL deionized water, which was replaced twice a day for 4 days, until all DMSO had been phase-inverted and all unreacted monomer was washed out. The removal of unreacted monomers was monitored by UV/VIS spectroscopy. The fully washed and swollen hydrogels were dried in an oven until all water had been removed and dry xerogels were obtained.

Preparation of G-DAT hybrid hydrogels

The synthesis of G-DAT hydrogels was carried out in a similar manner to the DAT hydrogels but in this case an organic dispersion of few-layer graphene (FLG) in DMSO was used instead of DMSO as the polymerisation medium. 0.1G-DAT and 0.5G-DAT hydrogels were prepared from 0.1% w/w (0.42 mg mL^{-1}) and 0.5% w/w (2.1 mg mL^{-1}) FLG loadings, respectively.

Scanning electron microscopy (SEM) imaging

The samples were prepared by swelling the hydrogels until their maximum swelling state followed by freezing. The samples were then lyophilised in a Telstar Lyoquest freeze dryer to remove all water from the hydrogel. The porous microstructure of the samples was analysed by SEM imaging using a Gemini SEM 500 from Zeiss. Freeze-dried samples were placed in a sample-holder and introduced onto the microscope stage for imaging at an accelerating voltage of 2–3 kV. Pore size distributions were obtained by plotting the average pore sizes of several digital images for each sample.

BET analysis

The specific surface area, pore diameter and pore volume of DAT hydrogels were measured with a Quantachrome NOVA TOUCH 2LX instrument at 77 K. Prior to investigation, freeze-dried hydrogels were degassed under vacuum at 100 °C for 5 h.

TGA studies

The fully swollen hydrogels were frozen and lyophilized in a Telstar Lyoquest freeze dryer. The samples were then analyzed on a Q50 system from TA instruments at 10 °C min^{-1} under an N_2 atmosphere. Each sample was analysed in triplicate.

SDT (simultaneous DSC-TGA)-MS

The fully swollen hydrogels were frozen and lyophilized in a Telstar Lyoquest freeze dryer. The samples were then analysed

on a Simultaneous DSC-TGA QSeries instrument (SDT Q600) from TA instruments at 10 °C min^{-1} under an N_2 atmosphere. The SDT was coupled to a mass spectrometer for evolved gas analysis (EGA). Each sample was analysed in triplicate.

Swelling studies

Swelling studies were performed using a gravimetric method, by immersing dried hydrogel pieces in ultrapure water or SGF medium at room temperature. The samples were initially weighed so that the average initial weights were similar (~7 mg). The weights were recorded at defined time intervals until the hydrogel samples reached a constant weight. Prior to weighing, the samples were placed on filter paper to remove excess water. The swelling degree (SD) was then calculated according to the following equation:

$$\mathrm{SD} = \frac{W_t - W_0}{W_0}$$

where W_0 and W_t are the initial weigh and weight at time t, respectively. Three samples were weighed for each measurement.

Mechanical properties

Compressive and tensile tests were carried out with a Mecmesin Multitest 2.5-i dynamic mechanical analyser at room temperature. For compressive studies, samples were cylindrical disks prepared from silicon moulds with initial diameters and thicknesses of 1.05 cm and 1 cm, respectively. Hydrogel samples were then uniaxially compressed between two plates at a rate of 6 mm min^{-1} and a cell load of 50 N. Young's modulus values were recorded in terms of strain (which equals to the percentage ratio of the initial height of the sample to the final height of the sample) and these were in the range 2–10%. Fatigue tests were carried out by performing 100 compressive cycles with a rate of 40 mm min^{-1} and a 50 N cell load. Tensile test probes were prepared from silicon moulds that met the ISO 37 standard. Samples were uniaxially stretched at 60 mm min^{-1} with a 50 N cell load until the probe broke. The fracture toughness was calculated from the area under the stress–strain curves.

In vitro drug loading studies

Dried hydrogel samples were immersed in a 0.002 M solution of the corresponding drug in PBS for 4 days at room temperature until maximum swelling had occurred. For separate studies of Imipramine release, a 0.009 M (2.5 mg mL^{-1}) solution of Imipramine hydrochloride in PBS was used. Loaded hydrogels were then briefly washed with 2 mL of PBS buffer to remove unloaded drug from the surface of the samples, and the washings were collected with the remaining unloaded solution. The drug loading was then calculated by an indirect method:

$$\text{Drug loading}(\%) = \left(\frac{m_0 - m_u}{m_0}\right) \times 100$$

where m_0 is the total initial mass present in the loading medium and m_u is the mass of the unloaded drug remaining after the hydrogel had incorporated the drug. The drug loading was quantified by UV/VIS spectrophotometric analysis at a specific wavelength according to each drug solution, with the absorbances interpolated in a calibration curve, according to the Lambert–Beer law (Fig. S1 and S2†). Each measurement was carried out in duplicate.

In vitro drug release studies

The drug-loaded hydrogels were immersed in 50 mL of buffered media. The samples were placed in an orbital mixer and shaker with a heating platform (ROTATERM 3000435 JP SELECTA) operating at 70 rpm and 37 °C. The study was carried out separately in both PBS (phosphate buffer saline, pH = 7.4) and SGF media. At defined time intervals, aliquots of 5 mL were withdrawn and replaced with the same volume of fresh buffer, so that the volume of the release medium remained constant. The aliquots were quantified by UV/VIS spectrophotometric analysis with interpolation in calibration curves following the Lambert–Beer law. Each measurement was carried out in duplicate, and the average release profile was obtained.

Results and discussion

Synthesis of (G)-DAT hydrogels

The synthesis of DAT-based hydrogels was carried out by *in situ* radical polymerisation in DMSO. VDAT, OEGMA, AM, MBA and KPS were dissolved in the solvent with stirring and the solution was sonicated. The mixture was cast in pre-heated silicon moulds and samples were heated for 20 min in an oven at 70 °C. The hybrid G-DAT hydrogels were fabricated in a similar way by previously preparing a homogeneous organic dispersion of few layer graphene (FLG) in DMSO, followed by the addition of the other reactants. The resultant organogels were washed thoroughly in water, in which DMSO is phase-inverted and all unreacted monomer is washed out, to give DAT and G-DAT hybrid hydrogels (Fig. 1). Importantly, the nanomaterial did not leak out of the hydrogel after washings and it remained embedded in the polymeric structure, as reported for the previous preparation of hybrid hydrogels by our group.[25]

Few-layer graphene was obtained by a mechano-chemical exfoliation process in the presence of melamine[21,26] (see ESI†). We performed theoretical and experimental studies that show how the interaction of diaminotriazines with graphitic layers facilitates the exfoliation, due to π–π favourable and graphene-NH_2 interactions between diaminotriazines and graphene layers.[19,20] Based on these premises, a diaminotriazine matrix-based hydrogel was designed for which it was envisaged that graphene would establish similar interactions. The preservation of the intrinsic sp^2 nature of the nanomaterial is therefore of critical importance. In order to meet this condition, few-layer graphene was used with a low amount of defects, as

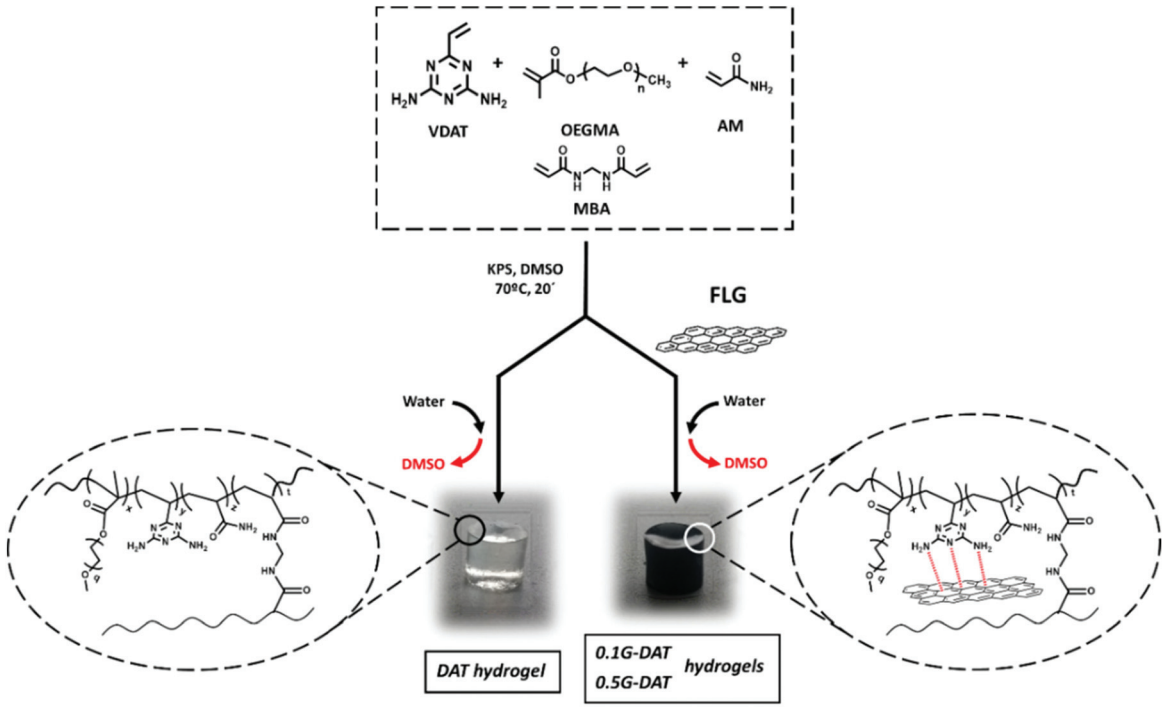

Fig. 1 Synthesis of DAT and G-DAT hydrogels.

indicated by Raman spectroscopy, with an I_D/I_G ratio of 0.38 and a number of layers $N_G = 4$.[27] A low percentage of oxygen was also observed (4% oxygen content measured by elemental analysis) and this is consistent with TGA data. Further TEM images are also provided (Fig. S3†).

Swelling studies

The swelling behaviour of a hydrogel defines the amount of water that can be held inside the porous structure of the network. This is quantified by the swelling degree (SD), which depends on several parameters such as pore and mesh sizes, density of crosslinking, functional hydrophilicity, and polymer concentration in the hydrogel.

Diaminotriazine-based hydrogels are pH-sensitive as DAT molecules can be protonated in strongly acidic media.[10] In the body, such harsh acidic conditions occur in the stomach, where a low pH and other substances are crucial for the process of digestion. Simulated gastric fluid (SGF), (pH = 1.2) is often used as a buffer to mimic the acidic environment in the gut,[28] where DAT-based hydrogels could serve as pH-sensitive drug reservoirs. Therefore, in this study the swelling properties of the hydrogels in both water and SGF were measured. The results show that swellings up to 10-fold greater were observed in acidic media in comparison to aqueous media (Fig. 2a). As would be expected, when the pH drops below the pK_a of VDT (pK_a = 5.15)[10] the DAT molecules become protonated and repel each other due to cationic repulsive forces (DAT+), and the polymeric network is forced to expand, thus allowing higher contents of water than at neutral pH.[29]

Interestingly, a trend was observed where increasing graphene content (G%) resulted in higher SD values in both neutral and acidic media (Fig. 2a, and inset), thus suggesting that graphene is exerting a distinctive effect in the polymeric network. In an effort to understand this effect, a possible mechanism for the swelling of (G)-DAT hydrogels is depicted in Fig. 2b–d. In DAT hydrogels the hydrophobic interactions govern the swelling degree, due to the presence of the DAT core. In aqueous neutral media, triazine molecules are known to self-assemble into hydrophobic microdomains through DAT–DAT hydrogen bonding and π–π stacking interactions[9] (Fig. 2b, depicted in red and blue, respectively). These microdomains act as a "hydrophobic barrier" for small protic molecules like water, thus restraining water uptake. As mentioned earlier, when graphene is introduced, favourable π–π stacking is likely to occur between triazine molecules and graphene sheets (πG–πDAT), together with NH_2-graphene interactions.[19,20] These graphene-diaminotriazine engagements may disrupt DAT–DAT stacking to a certain extent, thus loosening the tight DAT hydrophobic microdomains. Consequently, more water is allowed into the network (Fig. 2c).

In acidic media DAT hydrogels increase their SD 10-fold (Fig. 2a). When, additionally, G-DAT hybrid hydrogels are immersed in SGF buffer, cationic repulsion between DAT molecules breaks the tight DAT H-bonding network, and this leads to a marked increase in SD (Fig. 2d) and also changes the absorption energy of DAT on graphene, which is related to the ability of DATs to accept charge transfer from the latter.[19] These swelling behaviours can both be observed macroscopically for both DAT and G-DAT hybrid hydrogels in neutral and

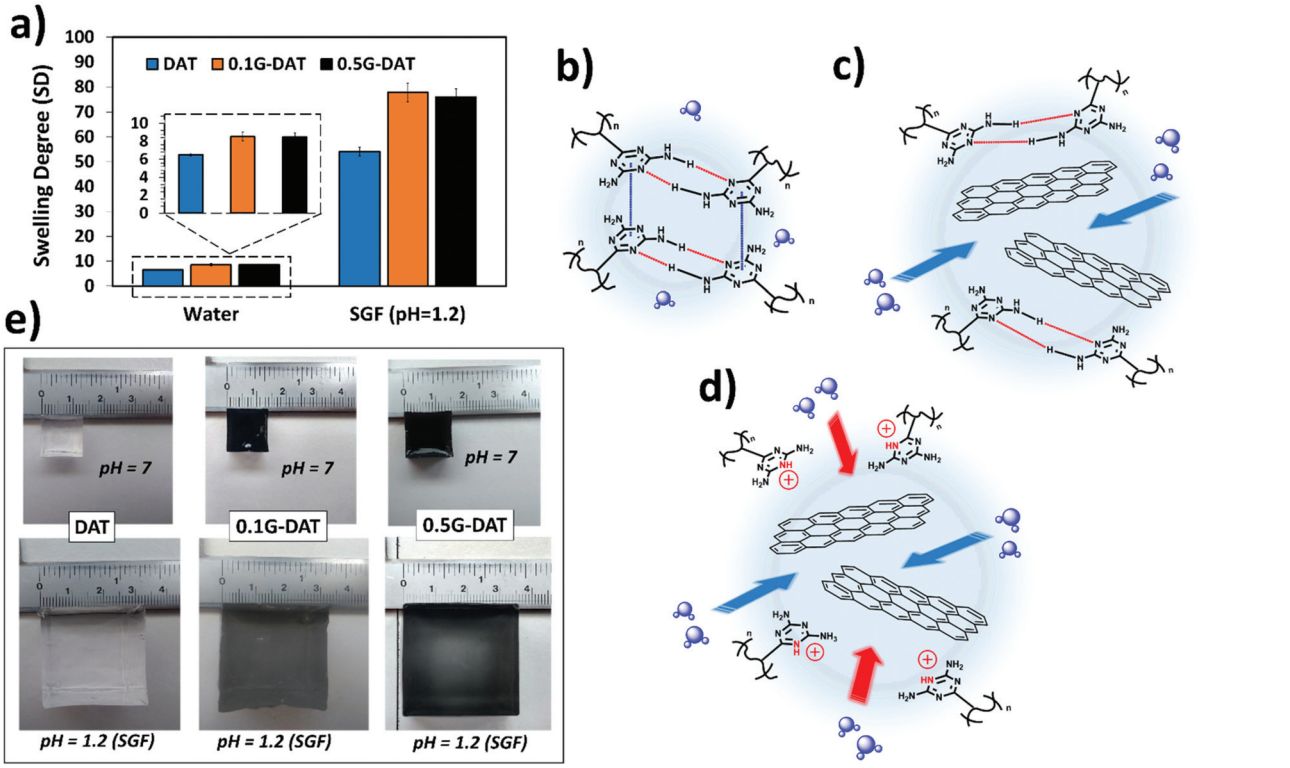

Fig. 2 (a) Swelling degree in water and SGF of DAT-based hydrogels. Proposed swelling mechanism for (b) DAT hydrogels in neutral media (c) hybrid G-DAT hydrogels in neutral media and (d) G-DAT hydrogels in SGF media (e) digital images of fully swollen hydrogels.

acidic media (Fig. 2e). It is worth noting that, despite the fact that the DAT backbone is disrupted, the presence of acrylamide (AM) keeps the hydrogel from losing consistency in acidic media and this is due to weak amide–amide H-bonding.

TGA/DSC-MS studies

The TGA of the DAT-based hydrogels in neutral media was carried out to corroborate the results discussed above. Several peaks corresponding to different weight losses can be distinguished (Fig. 3). The most relevant peaks are observed at around 390 °C and these presumably correspond to decomposition of the polymeric backbone (Fig. 3, inset).

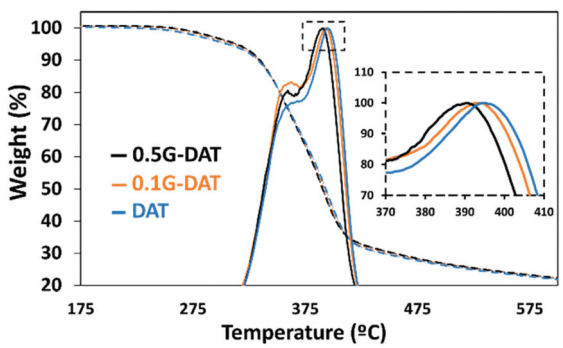

Fig. 3 TGA curves (dashed lines) and derivatives (solid lines) for (G)-DAT hybrid hydrogels.

Moreover, the simultaneous thermal analysis (SDT) was carried out in order to study the decomposition profiles of the hydrogels (Fig. S4a†). Two main weight losses can be appreciated in the TGA derivatives (blue, orange and black solid lines): a small 7.4% loss is observed during the first 100 °C whereas a major loss of 60.8% occurs in the range 300–450 °C. coupled mass spectrometry for gas analysis revealed that the first loss corresponds to the water that remained in the hydrogels (Fig. S4a,† red, purple and green). The second major loss shows a carbon dioxide peak at 425 °C (Fig. S4b,† red, purple and green) and this corresponds to the main decomposition of the polymer backbone.

DSC provided the energy profile following pyrolysis of the hydrogels (Fig. S4c,† red, purple, green): a downward trend is observed up to 300 °C, which indicates that heat is essentially absorbed by the material at lower temperatures. A shift in the DSC profile from 300–450 °C, with a maximum at 430 °C, shows that the decomposition of the polymer backbone is exothermic. It is noteworthy that 0.5G-DAT hybrids show less marked rises in energy profiles than DAT and 0.1G-DAT hydrogels, as shown in the DSC (Fig. S4c,† green), proving that less energy is involved in the decomposition of the material at higher graphene contents. This finding is consistent with the difference in temperatures observed at the maxima of the TGA derivatives (Fig. S4d†): on increasing the amount of graphene, the decomposition of the backbone shifts to lower temperatures.

Both findings are consistent with a loosening of the polymeric network, as. graphene exerts a disruptive effect between the DAT units that control the structure of the hydrogel.

SEM studies

SEM imaging provided the pore size distributions of (G)-DAT hydrogels in their maximum swollen states in both neutral and acidic media. In neutral media (PBS) the DAT hydrogels had very heterogeneous pore sizes (15 ± 14.5 μm) and pore polydispersity (Fig. 4, blue). A notable narrowing in the pore size was observed in 0.1G-DAT and 0.5G-DAT hybrids (4.37 ± 0.45 μm and 3.99 ± 0.51 μm, respectively) and this led to sharper distributions (Fig. 4, orange and black, respectively).

Digital SEM images show a decrease in the heterogeneity of the pores as the graphene content was increased and the pore sizes became more similar (Fig. 5a–c). This gradual homogenisation of the pore size with the increase in G% can be attributed to the increasing πG–πDAT interactions: DAT molecules form extended 2D hydrogen-bonded films on top of the graphene surface and this may rearrange the typical amorphous porosity attributed to tight DAT–DAT aggregation.[30]

In SGF media the pore sizes increase 10-fold with respect to the neutral media, whereas the pore size distributions are broader and somewhat similar, with only a slight narrowing of the pore size observed when graphene is incorporated (Fig. 4, dashed blue, orange and black). When the H-bonding network is disrupted upon protonation, the DAT aggregates loosen and the pore expands, consequently decreasing the pore heterogeneity observed in neutral media, attributed to DAT–DAT aggregation. The presence of graphene in this medium therefore does not significantly rearrange the pore sizes of the hydrogels, as can be observed in the SEM digital images (Fig. 5d–f). Further BET characterization is provided in Fig. S5.†

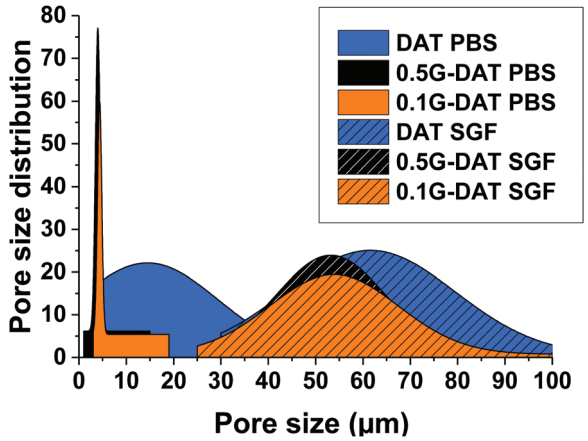

Fig. 4 SEM pore size distributions of (G)-DAT hydrogels in PBS and simulated gastric fluid.

Mechanical properties

G-DAT hybrid hydrogels consist of a terpolymeric network embedded with FLG. VDAT (2-vinyl-4,6-diamino-1,3,5-triazine) serves as a hydrophobic monomer that strengthens the network *via* strong DAT–DAT non-covalent interactions, namely hydrogen bonding and π–π stacking interactions, whereas OEGMA is used as a hydrophilic counterpart to offset this hydrophobicity (Fig. S6a†). The role of AM in these hydrogels is twofold: in neutral media this monomer acts as a reversible physical crosslinker by complementing strong DAT–DAT hydrogen bonding. This helps to dissipate energy when the system is subjected to an external load,[31] consequently leading to tougher hydrogels.[32] On the other hand, AM provides mechanical stability in acidic media through amide–amide hydrogen bonds after the complete breakdown of DAT–DAT hydrogen bonds upon protonation. This keeps the hydrogel from otherwise losing shape and consistency in SGF media (Fig. S6b†).

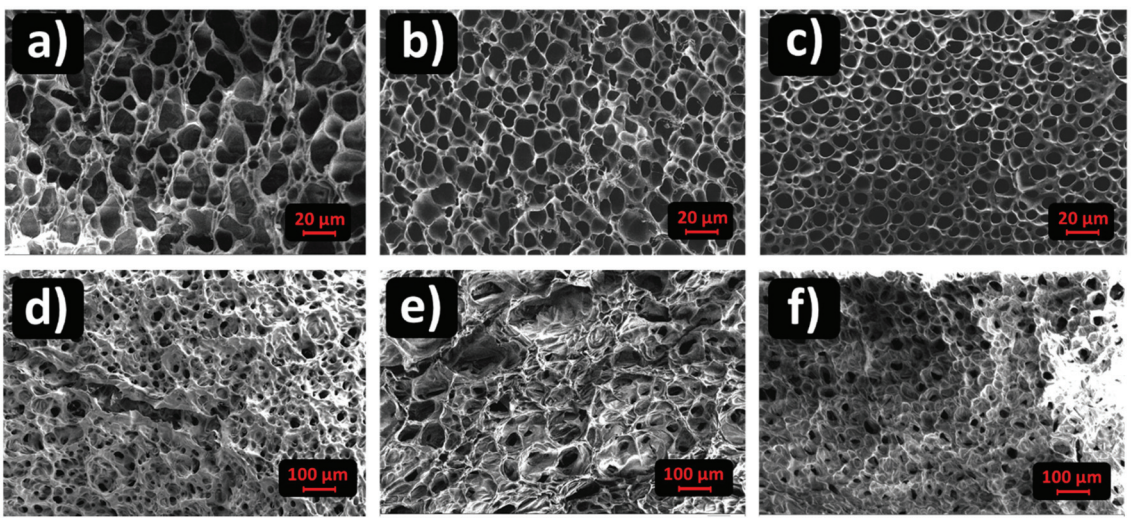

Fig. 5 Porous morphology of (G)-DAT hydrogels in PBS media for (a) DAT, (b) 0.1G-DAT, (c) 0.5G-DAT and for (d) DAT, (e) 0.1G-DAT and (f) 0.5G-DAT in SGF media.

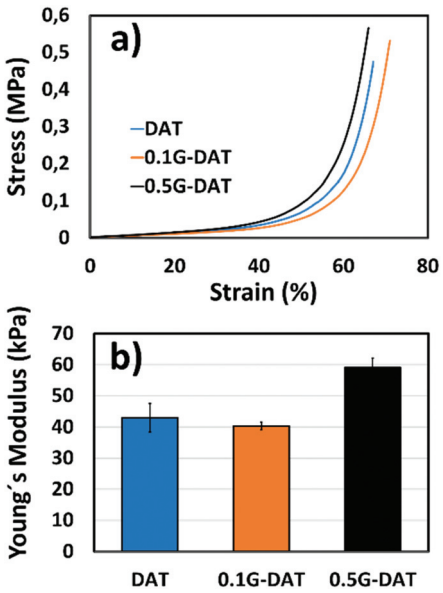

Fig. 6 Compressive studies for (G)-DAT hydrogels (a) stress–strain curves (b) Young's modulus.

In the compression study the elastic modulus initially dropped from 43 to kPa to 40 kPa in 0.1G-DAT hybrids, whereas the value increased back to 59 kPa when the level of graphene was increased in 0.5G-DAT hydrogels (Fig. 6b).

This opposite trend can be rationalized if we first consider the non-covalent interactions that are present in DAT-based hydrogels. It has been reported that upon increasing the VDAT content in VDAT-based hydrogels a significant increase in the elastic modulus is observed as a consequence of the growing formation of rigid DAT hydrophobic microdomains.[29,30] When graphene is incorporated in 0.1G-DAT hydrogels, the triazine aggregates are disrupted to a certain extent due to the favorable πG–πDAT and NH_2-graphene interactions.[19,20]

Since the stiffness of VDAT-based hydrogels is caused by DAT aggregation, the introduction of graphene decreases the rigidity and increases the compressive strain in 0.1G-DAT hydrogels (Fig. 6a and b). In contrast, a further increase in graphene content, as in 0.5G-DAT hydrogels, leads to stiffer hydrogels. An increase in the G% content also implies a higher double bond activity, which in turn increases the crosslinking density in a polymerization medium and consequently the network rigidity,[33,34] despite the DAT aggregates are partially disrupted.

Tensile tests also provided evidence that graphene somehow disrupts the polymeric network to some extent. The introduction of 0.1% w/w graphene in DAT hydrogels decreases the tensile strength and toughness by 30% and 20%, respectively (Fig. S7a and b†), which suggests partial disruption of the DAT–DAT strengthening network. Nevertheless, 0.5G-DAT hybrids are tougher and more ductile despite the fact that the DAT network is compromised. We previously observed that an increase in G% loadings enhanced the tensile performance of graphene-based polymer hydrogels,[34]

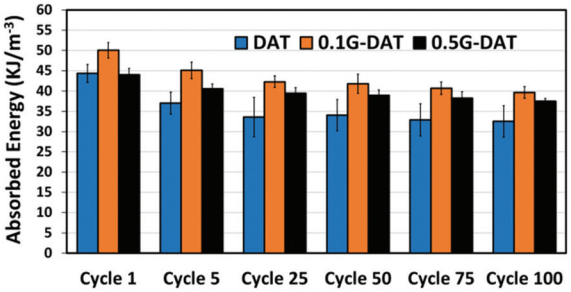

Fig. 7 100 cycle fatigue test for (G)-DAT hydrogels.

possibly due to an improvement in the load transfer throughout the network.[35,36]

Fatigue tests provided further evidence of the reinforcing effect of graphene in G-DAT hybrid hydrogels (Fig. 7). 0.1G-DAT hybrids absorbed higher energies throughout the 100 cycles than DAT hydrogels, which is consistent with a more elastic network brought about by the disruptive effect of the πG–πDAT interactions. In addition, G-DAT hybrids stand out for their antifatigue-like properties: only a 15% energy loss (energy dissipation between the 1st and 100th cycle) was observed for 0.5G-DAT hybrids, whereas 26% energy loss was observed for DAT analogues. This finding provides further evidence that graphene enhances the mechanical performance in G-DAT hydrogels. The results of the mechanical tests are provided in Table S1.†

In vitro drug loading/release studies

The incorporation of hydrophobic microenvironments into hydrophilic matrices is a useful strategy to host drugs with poor water solubility. As discussed in previous sections, the swelling response of (G)-DAT hydrogels is founded on the disruption of tight hydrophobic aggregates by the synergistic effect of graphene and the acidic medium. Following these premises, the disruption of the hydrophobic DAT domains that govern the hydrogel may be envisaged as a means to host and deliver hydrophobic drugs.

Firstly, to select an appropriate hydrophobic drug that could interact with the DAT matrix, a series of drugs of decreasing water solubility [Metronidazole (MZ), Benzocaine (BZ), Ibuprofen (IB), Naproxen (NX) and Imipramine (IMI)] were loaded into DAT hydrogels in equal amounts (Fig. 8a).

The results showed that low loadings of around 15% were observed for the hydrophilic drug MZ, whereas higher loadings were achieved for more hydrophobic drugs, particularly for IMI, which reached more than 35%. This suggests that the DAT matrix is suitable for hosting hydrophobic drugs within the porous hydrogel network. Previous studies suggest that poly(2-vinyl-4,6-diamino-1,3,5-triazine) (PVDAT) arranges into apolar microspheres, that exclude water from inside these domains and enable hydrophobic interactions between DAT residues.[10] These spheres could be acting as pockets to host the hydrophobic drugs within the polymer network of the DAT-based hydrogels. Copolymerisation with diaminotriazines

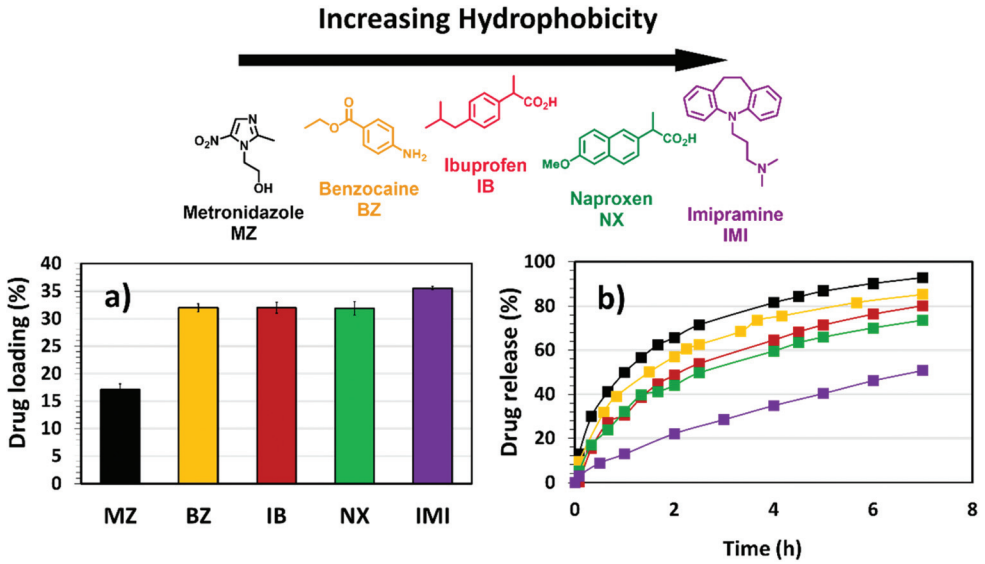

Fig. 8 *In vitro* (a) drug loading and (b) drug release of model drugs for DAT hydrogels in PBS. In order of decreasing water solubility: Metronidazole (MZ, black), Benzocaine (BZ, yellow), Ibuprofen (IB, red), Naproxen (NX, green) and Imipramine (IMI, purple).

could therefore provide a useful strategy to circumvent inefficient hydrophobic drug loading, which remains one of the main drawbacks in polymer drug delivery.[4]

Following loading into the DAT hydrogels, the drugs were allowed to diffuse through the network in PBS buffer solution (phosphate buffered saline, pH = 7.4) in the absence of any pH trigger (Fig. 8b). The diffusion profiles showed that, as the water solubility of the drug decreased (MZ, BZ, IB, NX, IMI, with the latter having the lowest water solubility) the drug release rate became slower. One would expect that a slower permeation of the drug through the network and out into the medium would be due to stronger interactions with the DAT matrix. The model drug Imipramine (IMI) showed a markedly slower permeation than the rest and this suggests a stronger drug-matrix affinity, as suggested by the loading studies. These findings provide evidence for the hydrophobic nature of the DAT-based hydrogel.

In order to evaluate the effect of graphene and an acidic medium on the delivery of hydrophobic drugs, model drug IMI was chosen for the subsequent *in vitro* loading/release studies. The drug loading capacities of (G)-DAT hydrogels for IMI are represented in Fig. 9. It can be seen that graphene slightly enhances the loadings of the model hydrophobic drug, probably due to the π–π stacking interactions between the graphenic surface and the small aromatic compound.[17,37]

The disruptive effect of graphene and environmental pH on the release of IMI was studied separately in two different buffered media, namely PBS (phosphate buffered saline, pH = 7.4) and SGF (simulated gastric fluid, pH = 1.2). In PBS media the model drug diffuses through the network in the absence of any pH trigger (Fig. 10a). In DAT hydrogels, however, IMI is released at a slow rate up to 60% of the payload and reaches a plateau after 24 hours, whereas G-DAT hybrids release 80% of the payload under similar conditions. It is clear that graphene speeds up the release rate of IMI, possibly due to the disrup-

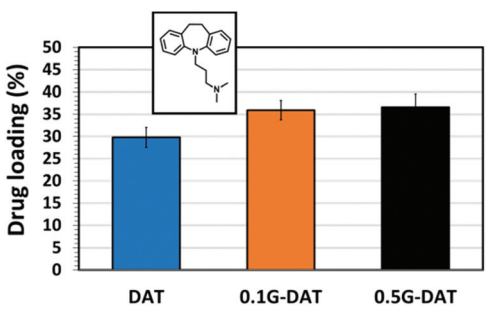

Fig. 9 *In vitro* drug loading of Imipramine in (G)-DAT hybrid hydrogels.

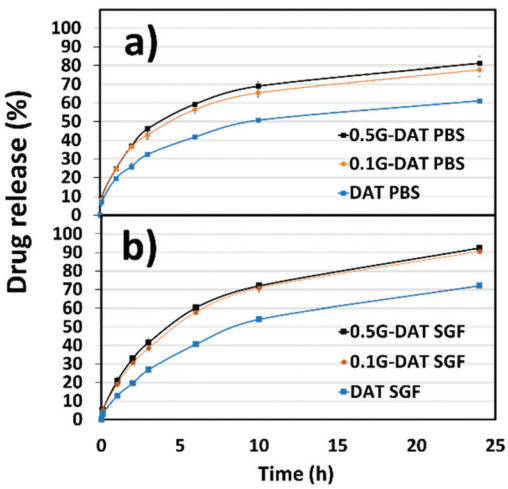

Fig. 10 *In vitro* pH-responsive drug release profiles of Imipramine for (G)-DAT hydrogels (a) in PBS (pH = 7.4) media and (b) SGF (pH = 1.2) media.

tive πG–πDAT interactions that interfere with hydrophobic DAT domains and favour the diffusion of the drug.

In SGF medium the release profiles of IMI appear steeper than those in PBS buffer and a plateau is not reached after 24 hours (Fig. 10b). In addition, both DAT and G-DAT hybrids in SGF release drug percentages 10% higher than their respective systems in PBS medium. The pore expansion that occurs in acidic media explains this improvement in the release profile. Moreover, G-DAT hybrids in this medium still retain higher release rates for IMI when compared with their DAT analogues, which highlights the positive influence of graphene on the release of drug, regardless of the external pH.

After 24 hours, a 30% improvement in the release was observed for the 0.5G-DAT hybrids immersed in SGF media when compared with their DAT gel counterparts immersed in PBS (Fig. S8†). This result demonstrates the synergistic effect of the disruptive interactions that graphene and the acidic pH exert on the drug release: a combination of the two effects relieves strain in the network and increases the pore size, thus facilitating the release of the compound. These findings suggest that specific interactions between graphene and an appropriate polymer matrix can trigger the release of a hydrophobic drug from a soft scaffold.

Conclusions

We report herein the preparation of novel diaminotriazine (DAT) and graphene-diaminotriazine (G-DAT) hybrid hydrogels as soft scaffolds for the delivery of hydrophobic drugs. The dual nature of the hybrids confers them with both mechanical robustness and stimuli responsiveness. The DAT heterogeneous aggregates increase the hydrophobic character of the hydrogel and its affinity for hydrophobic drugs, while also imparting pH responsiveness. On the other hand, graphene homogenizes the internal structure of the hydrogel, enhances the mechanical and swelling properties and improves the loading and release capacities. It has been demonstrated here that graphene provides an unprecedented non-covalent means to deliver a hydrophobic drug by disrupting the hydrophobic interactions that govern the hydrogel. In addition, the external pH acts synergistically to improve the release through expansion of the DAT residues. These novel proof-of-concept hydrogels expand the scope of graphene in the delivery of therapeutic agents by non-covalent interactions.

Conflicts of interest

There are no conflicts to declare.

Acknowledgements

The authors acknowledge financial support from the European Union's Graphene-based disruptive technologies, Flagship project GA785219 Graphene core 2, European FEDER UNCM15-CE-2839, the Spanish government (project CTQ2014-53600-R and project CTQ2017-88158-R), and Junta de Comunidades de Castilla-La Mancha (project SBPL4/17/180501/000204). J. L. B. acknowledges the Spanish Ministry of Economy and Competitiveness (MINECO) for his grant (BES2015-074218).

References

1 S. Garg, A. Garg and R. D. Vishwavidyalaya, *Asian J. Biomater. Res.*, 2017, **2**, 163–170.
2 S. Naahidi, M. Jafari, M. Logan, Y. Wang, Y. Yuan, H. Bae, B. Dixon and P. Chen, *Biotechnol. Adv.*, 2017, **35**, 530–544.
3 J. Li and D. J. Mooney, *Nat. Rev. Mater.*, 2016, **1**, 16071.
4 E. Larrañeta, S. Stewart, M. Ervine, R. Al-Kasasbeh and R. F. Donnelly, *J. Funct. Biomater.*, 2018, **9**, 13.
5 M. McKenzie, D. Betts, A. Suh, K. Bui, L. D. Kim and H. Cho, *Molecules*, 2015, **20**, 20397–20408.
6 R. Mateen and T. Hoare, *J. Mater. Chem. B*, 2014, **2**, 5157–5167.
7 B. Gidwani and A. Vyas, *BioMed Res. Int.*, 2015, 15.
8 T. J. Mooibroek and P. Gamez, *Inorg. Chim. Acta*, 2007, **360**, 381–404.
9 K. E. Maly, C. Dauphin and J. D. Wuest, *J. Mater. Chem.*, 2006, **16**, 4695.
10 H. Asanuma, T. Ban, S. Gotoh, T. Hishiya and M. Komiyama, *Macromolecules*, 1998, **31**, 371–377.
11 Y. Wang, L. Li, N. Shao, Z. Hu, H. Chen, L. Xu, C. Wang, Y. Cheng and J. Xiao, *Acta Biomater.*, 2015, **17**, 115–124.
12 N. Shao, H. Wang, B. He, Y. Wang, J. Xiao, Y. Wang, Q. Zhang, Y. Li and Y. Cheng, *Biomater. Sci.*, 2015, **3**, 500–508.
13 Z. Cao, W. Liu, D. Liang, G. Guo and J. Zhang, *Adv. Funct. Mater.*, 2007, **17**, 246–252.
14 P. Wang, J. Zhang, Y. Li, N. Wang and W. Liu, *Mater. Lett.*, 2015, **142**, 71–74.
15 A. K. Geim, *Science*, 2009, **324**, 1530–1535.
16 J. M. Allen, T. C. Vincent and K. B. Richard, *Chem. Rev.*, 2010, **110**, 132–145.
17 R. Cavalli, M. Soster and M. Argenziano, *Ther. Delivery*, 2016, **7**, 117–138.
18 Z. Chen and H. Lu, *J. Mater. Chem.*, 2012, **22**, 12479–12490.
19 V. León, A. M. Rodríguez, P. Prieto, M. Prato and E. Vázquez, *ACS Nano*, 2014, 563–571.
20 A. M. Rodríguez, A. B. Muñoz-García, O. Crescenzi, E. Vázquez and M. Pavone, *Phys. Chem. Chem. Phys.*, 2016, **18**, 22203–22209.
21 J. M. González-Domínguez, V. León, M. I. Lucío, M. Prato and E. Vázquez, *Nat. Protoc.*, 2018, **13**, 495–506.
22 Q. Wang, Y. Zhang, X. Dai, X. Shi and W. Liu, *Sci. China: Technol. Sci.*, 2017, **60**, 78–83.
23 H. Gao, N. Wang, X. Hu, W. Nan, Y. Han and W. Liu, *Macromol. Rapid Commun.*, 2013, **34**, 63–68.
24 N. Sawa and T. Masuda, *Japan Pat*, 853059541, 1987.

25 C. Martín, A. Martín-Pacheco, A. Naranjo, A. Criado, S. Merino, E. Díez-Barra, M. A. Herrero and E. Vázquez, *Nanoscale*, 2019, 4822–4830.
26 V. León, J. M. González-Domínguez, J. L. G. Fierro, M. Prato and E. Vázquez, *Nanoscale*, 2016, **8**, 14548–14555.
27 K. R. Paton, E. Varrla, C. Backes, R. J. Smith, U. Khan, A. O'Neill, C. Boland, M. Lotya, O. M. Istrate, P. King, T. Higgins, S. Barwich, P. May, P. Puczkarski, I. Ahmed, M. Moebius, H. Pettersson, E. Long, J. Coelho, S. E. O'Brien, E. K. McGuire, B. M. Sanchez, G. S. Duesberg, N. McEvoy, T. J. Pennycook, C. Downing, A. Crossley, V. Nicolosi and J. N. Coleman, *Nat. Mater.*, 2014, **13**, 624–630.
28 D. Guérin, J. C. Vuillemard and M. Subirade, *J. Food Prot.*, 2003, **66**, 2076–2084.
29 L. Tang, W. Liu and G. Liu, *Adv. Mater.*, 2010, **22**, 2652–2656.
30 J. Zhang, N. Wang, W. Liu, X. Zhao and W. Lu, *Soft Matter*, 2013, **9**, 6331.
31 B. Xu, Y. Zhang and W. Liu, *Macromol. Rapid Commun.*, 2015, **36**, 1585–1591.
32 X. Zhao, *Soft Matter*, 2014, **10**, 672–687.
33 C. Martín, S. Merino, J. M. González-Domínguez, R. Rauti, L. Ballerini, M. Prato and E. Vázquez, *Sci. Rep.*, 2017, **7**, 10942.
34 J. M. González-Domínguez, C. Martín, Ó. J. Durá, S. Merino and E. Vázquez, *ACS Appl. Mater. Interfaces*, 2018, **10**, 1987–1995.
35 M. Wang, C. Yan and L. Ma, in *Composites and Their Properties*, ed. N. Hu, InTech, Croatia, 2012, ch. 2, pp. 17–36.
36 R. J. Young, I. A. Kinloch, L. Gong and K. S. Novoselov, *Compos. Sci. Technol.*, 2012, **72**, 1459–1476.
37 V. Georgakilas, J. N. Tiwari, K. C. Kemp, J. A. Perman, A. B. Bourlinos, K. S. Kim and R. Zboril, *Chem. Rev.*, 2016, **116**, 5464–5519.